

# “Multipoint Force Feedback” Leveling of Massively Parallel Tip Arrays in Scanning Probe Lithography

Hanul Noh, Goo-Eun Jung, Sukhyun Kim, Seong-Hun Yun, Ahjin Jo, Se-Jong Kahng, Nam-Joon Cho,\* and Sang-Joon Cho\*

**N**anoscale patterning with massively parallel 2D array tips is of significant interest in scanning probe lithography. A challenging task for tip-based large area nanolithography is maintaining parallel tip arrays at the same contact point with a sample substrate in order to pattern a uniform array. Here, polymer pen lithography is demonstrated with a novel leveling method to account for the magnitude and direction of the total applied force of tip arrays by a multipoint force sensing structure integrated into the tip holder. This high-precision approach results in a  $0.001^\circ$  slope of feature edge length variation over 1 cm wide tip arrays. The position sensitive leveling operates in a fully automated manner and is applicable to recently developed scanning probe lithography techniques of various kinds which can enable “desktop nanofabrication.”

H. Noh, G.-E. Jung, S. Kim, S.-H. Yun, A. Jo,  
Dr. S.-J. Cho

Research and Development Center  
Park Systems

Suwon 443-270, South Korea  
E-mail: msjcho@snu.ac.kr

G.-E. Jung, Prof. S.-J. Kahng  
Department of Physics  
Korea University

Seoul 136-713, South Korea

Prof. N.-J. Cho  
School of Materials Science and Engineering  
Nanyang Technological University  
50 Nanyang, Avenue, 639798, Singapore  
E-mail: njcho@ntu.edu.sg

Prof. N.-J. Cho  
Centre for Biomimetic Sensor Science  
Nanyang Technological University  
50 Nanyang Drive, 637553, Singapore

Prof. N.-J. Cho  
School of Chemical and Biomedical Engineering  
Nanyang Technological University  
62 Nanyang, Drive, 637459, Singapore

Dr. S.-J. Cho  
Advanced Institute of Convergence Technology  
Seoul National University  
Suwon 443-270, South Korea

DOI: 10.1002/sml.201403736



## 1. Introduction

Scanning probe lithography (SPL)<sup>[1]</sup> enables high resolution patterning with a sharp tip in close proximity to a sample surface. The atomic force microscope (AFM)<sup>[2]</sup> is commonly employed in SPL due to the nanoscale patterning capabilities of diverse materials,<sup>[3]</sup> e.g., dip-pen nanolithography (DPN)<sup>[4]</sup> which is widely used to precisely deposit molecular inks on a variety of sample substrates. For a large area duplication of patterns, DPN with 2D tip arrays<sup>[5]</sup> and low-cost cantilever-free SPL methods using polymer pen lithography (PPL),<sup>[6]</sup> beam pen lithography (BPL),<sup>[7]</sup> and hard-tip soft-spring lithography (HSL)<sup>[8]</sup> have been successfully demonstrated across centimeter scale areas. In particular, a recent report by Liao et al. shows that large area SPL can be adopted as a desktop nanofabrication platform for rapid prototyping of functional electronic devices.<sup>[9]</sup> As patterning areas get wider in SPL, leveling, i.e., maintaining tip alignment with respect to a sample surface has remained a considerable challenge. In order to achieve leveling accuracy and ease of use, novel methods have been proposed, including force feedback of polymer pen arrays (PPA),<sup>[10]</sup> dual-elastomeric materials approach of PPA,<sup>[11]</sup> self-leveling of dip pen arrays (DPA),<sup>[12]</sup> and optical alignment of perforated cantilever arrays.<sup>[13]</sup>

Herein, we describe a general leveling method which is independent of probe type, and hence applicable to a variety of SPL techniques for which tip arrays exert defined contact forces onto a sample surface. This leveling platform achieves both leveling accuracy and ease of use by means of “multipoint force feedback” and an automated leveling algorithm. As proof-of-principle, we demonstrate PPL patterning in  $1\text{ cm}^2$  region with a  $125 \times 125$  PPA. PPL is a molecular printing<sup>[14]</sup> method which uses thousands of elastomeric tips<sup>[15,16]</sup> to fabricate molecular patterns of diverse materials over a centimeter scale area.<sup>[17–19]</sup> In order to obtain inked patterns with consistent shape and dimension over a wide sample area, it is extremely important to control the two face angles between the PPA and sample substrate. The classical method of leveling utilized in PPL is to use an optical microscope vision<sup>[20]</sup> in order to check whether deformations of the PPA at the four corners are equivalent. The optical leveling method has a poor accuracy angle range of  $0.02^\circ$  due to the limitations of estimating tip contact conditions by optical microscope. In order to address this issue, Liao et al. reported a novel method to achieve  $0.004^\circ$  leveling precision by implementing a sensitive electric scale below the sample and by controlling the total force of PPA which is compressed with a fixed depth on the sample.<sup>[10]</sup> Xie et al. also reported another approach which is independent of the leveling instrument and works by implementing specialized “hard-apex, soft-base” tip arrays.<sup>[11]</sup> We expand upon and enhance the achievements demonstrated by Liao et al. in order to attain precise, easy, and quick leveling for extensive SPL techniques. This new “multipoint force feedback” leveling method measures both the magnitude of total force and the direction of the effective total applied force of the contacted tip arrays. These simultaneous measurements enable quick leveling, typically within 2 min for arbitrary tilt angles. Experimentally, this method comprises multipoint force sensors embedded into the tip holder and analytic calculation of the effective force position from the sensor signals.

## 2. Result and Discussion

In order to level various kinds of tip arrays exerting contact forces, a sensor block containing three low-profile force sensors (Honeywell, FSS1500NST) is integrated to a commercial AFM system (Park Systems, NX20). As shown in **Figure 1a**, the sensors are arranged into a triangular shape in order to make a kinematic mount capable of sustaining a stainless steel tip carrier by means of embedded magnets in the sensor block (see Figure S1, Supporting Information, for additional details). The tip carrier can be placed in the same position repeatedly due to the mounting holes on the tip carrier and point contacts of the three-point force sensors. In **Figure 1b**, an additional leveling setup is depicted. A homemade 2-axis tilting stage is inserted between a piezoelectric  $x$ – $y$  scanner and a sample positioning stage in order to adjust face angles in the  $x$ – $y$  direction. The step resolution of the tilting stage is  $7.7\text{ }\mu\text{rad}$  ( $0.00044^\circ$ ) which corresponds to  $<100\text{ nm}$  height difference across a  $1\text{ cm}$  distance. The sensor block, i.e., force-sensor-integrated tip holder is placed under a piezoelectric  $z$  scanner and a tip positioning  $z$  stage, and the forces acting on tip arrays are measured at three-point force sensors with respect to the  $z$  scanner and  $z$  stage positions during leveling or patterning processes. Any type of tip arrays exerting a certain force to the sensors can be attached on the tip carrier using commonly used double sided tape or adhesives. The integration of force sensors into the tip holder is a significant experimental improvement for a leveling platform since it enables simultaneous measurements of multipoint forces.

We employ polydimethylsiloxane (PDMS) pyramidal tip arrays<sup>[21]</sup> and conduct PPL patterning in order to demonstrate proof-of-principle for the new leveling method. The PPA was fabricated by a well-established protocol<sup>[20]</sup> and consists of  $125 \times 125$  (total 15 625) tips over  $1 \times 1\text{ cm}^2$  area. The shape of a tip is shown in **Figure 1b** circle, having a  $20\text{ }\mu\text{m}$  bottom width,  $w_b$ ,  $0.3\text{ }\mu\text{m}$  flattop width,  $w_t$ ,  $14\text{ }\mu\text{m}$  height,  $h$ , and  $80\text{ }\mu\text{m}$  pitch,  $d$ . All parameter values are based

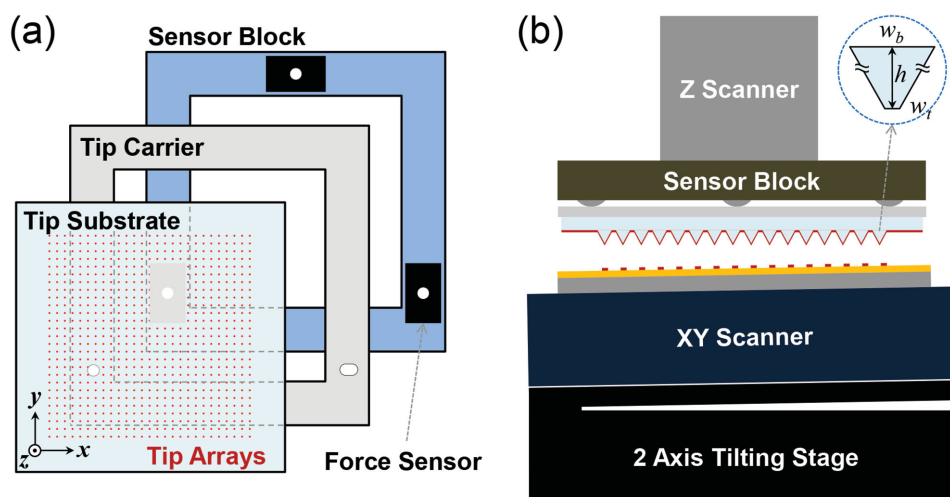


**Figure 1.** a) Position sensitive force sensing structures using a triangular kinematic mount of three-point force sensors. b) Experimental setup consisting of a  $7.7\text{ }\mu\text{rad}$  resolution 2-axis tilting stage, piezoelectric transducers, and a sensor block with polymer pen arrays.

on the original fabricated PPA design except  $w_t$  which is a measured value obtained by scanning electron microscopy (Figure S2, Supporting Information). To evaluate multipoint force feedback leveling, we introduce the effective position of PPA forces which can be derived theoretically from simple force and torque equations. The applied force of each compressed elastomeric tip is given by<sup>[22]</sup>

$$F_{ij} = \frac{wbw_t}{h} E(Z_{ij}) Z_{ij} \quad (1)$$

where  $Z$  is the compression depth,  $E$  is the elastic modulus which has two values of 1.38 and 8.97 MPa according to the compression depth,<sup>[22]</sup>  $i$  and  $j$  are the indices of each tip ranging from 0 to  $N - 1$  for  $x$  and  $y$  directions, respectively, and  $N$  is the number of tips in one direction, i.e., 125. Then, the total applied force is a summation of Equation (1) over all the tip arrays as expressed in the following equation

$$F = \sum_{i=0}^{N-1} \sum_{j=0}^{N-1} F_{ij} \quad (2)$$

If we consider an effective force which exerts on the position  $(X, Y)$  with total force  $F$ , the torque equations of equilibrium are represented as

$$|\tau_x| = \sum_{i=0}^{N-1} \sum_{j=0}^{N-1} y_j F_{ij} = F \cdot Y \quad (3)$$

$$|\tau_y| = \sum_{i=0}^{N-1} \sum_{j=0}^{N-1} x_i F_{ij} = F \cdot X \quad (4)$$

where  $\tau_x$  and  $\tau_y$  are torque elements of  $x$  and  $y$  coordinates, respectively. In Equation (4), the effective position of the total force in the  $x$  direction is given by

$$X = \sum_{i=0}^{N-1} \sum_{j=0}^{N-1} i \cdot d \cdot \left( \frac{F_{ij}}{F} \right) \quad (5)$$

The  $y$  position can be obtained in the same manner from Equation (3). If tip arrays and the sample substrate are not parallel, then one corner of the tip arrays touches the sample surface prior to the other parts, and  $(X, Y)$  is calculated as the position of contacted corner side. If the two planes are completely parallel, then the forces of all tips are the same so the force ratio of a tip is a constant  $F_{ij}/F = 1/N^2$  which means that the effective force position becomes the center of the tip arrays

$$X_{\text{leveled}} = \frac{d}{N^2} \sum_{i=0}^{N-1} \sum_{j=0}^{N-1} i = \frac{d(N-1)}{2} \quad (6)$$

Therefore, leveling can be done by obtaining the effective force coordinates and adjusting the tilting stage angles to fit  $(X, Y)$  into the center position of tip arrays.

In order to quantitatively understand the leveling concept, theoretical calculations on the  $125 \times 125$  PDMS PPA are performed. When one edge of the PPA contacts the sample surface and the  $z$  scanner is extended by a certain length, a part of the PPA is pressed and applies forces on the sample surface. With a given set of conditions, the total force and effective position are obtained by Equations (2) and (5), respectively. Simulation results are shown in **Figure 2** with various tilt angles. In the simulation, the

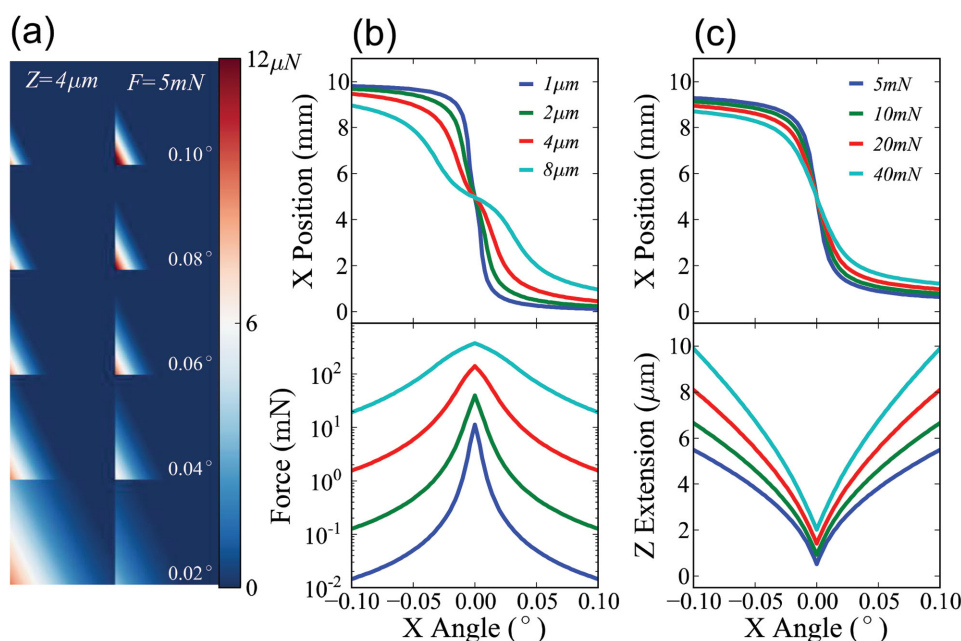


**Figure 2.** Theoretical simulations on the leveling concept of PDMS PPA. a) Force mapping images of partially pressed PPA with constant depth (left) and constant total force (right) according to the tilt angle. b) Position (upper) and magnitude (lower) variations of effective force with respect to the  $z$  scanner extension. c) Position (upper) of effective force and  $z$  scanner extension (lower) variations with respect to the total applied forces.

$y$  tilt angle is simultaneously changed as half of the  $x$  tilt angle so that the  $x$  angle is only represented in Figure 2. In Figure 2a, 2D force maps of partially compressed PPA are shown as 5 by 2 subplots at the same color scale with given tilt angle,  $z$  scanner extension (left column), and total force (right column). Once the extension length is kept constant, then the total force increases as the tilt angle decreases. Thus, the total force curve has a peak if the tilt angles are swept through leveling point.<sup>[10]</sup> This is shown in Figure 2b lower part with various extension lengths. When the total force is kept at constant, the  $z$  extension length curve has a dip as shown in Figure 2c lower part. By observing the force maximum in the constant extension case or the extension minimum in the constant force case, leveling can be accomplished. However, these methods require quite many iterations in both the  $x$  and  $y$  directions in order to achieve high resolution leveling. Furthermore, the total force of the tip arrays must be larger than the experimentally measurable level. If the tip arrays exert an unmeasurable force on the sample surface, they are difficult to use. On the other hand, the effective force position theoretically calculated from Equation (5) make it possible to reduce iteration counts and use small force tip arrays. Simulated position ( $X$ ) traces of the effective force are shown in the upper part of Figure 2b,c for constant extension and constant force cases, respectively. Since one corner of the PPA was set to the origin and the size of the PPA is 1 cm, the effective force position of leveling point is 5 mm. In Figure 2b,c,  $X$  position curves approach to this center position when the tilt angle decrease. Because the shapes of tip arrays are typically rectangular, the center position of the PPA can be easily defined and measured in experiments. By measuring the difference between the current effective force position and center position of tip arrays, we can obtain the quantity and direction of tilt angles in both the  $x$  and  $y$  directions simultaneously. If we measure the tilting amount and direction exactly, leveling can be done with just one adjustment of the tilting stage. From an experimental point of view, this is quite difficult because there are various shapes of the effective force position curves according to the sort and contact conditions of tip arrays. Therefore, we used only the direction information in order to adjust the tilt angles in the leveling experiment. Although the quantity information of the tilt angle is disregarded, it is possible to significantly reduce iteration counts by employing a root finding algorithm such as the bisection method, because of the directional information and monotonic response of the effective force position.

Additionally, if there exists guide structures around the tip arrays,<sup>[12]</sup> then this method can be applied to level various kinds of tip arrays with experimentally unmeasurable small forces.

Implementation of multipoint force feedback leveling with direction information is achieved by three sensitive force sensors as shown in Figure 3a. Three force sensors ( $F_1, F_2, F_3$ ) and the effective force  $F$  are depicted as blue dots and a red dot, respectively. From the theoretical equations, the force and torque equations are given as

$$F = F_1 + F_2 + F_3 \quad (7)$$

$$F \cdot X = b \cdot (F_3 - F_2) \quad (8)$$

$$F \cdot Y = a \cdot F_1 - c \cdot (F_2 + F_3) \quad (9)$$

where  $a, b$ , and  $c$  are dimension factors of the three force sensors. Arranging the equations, the effective force position is given by

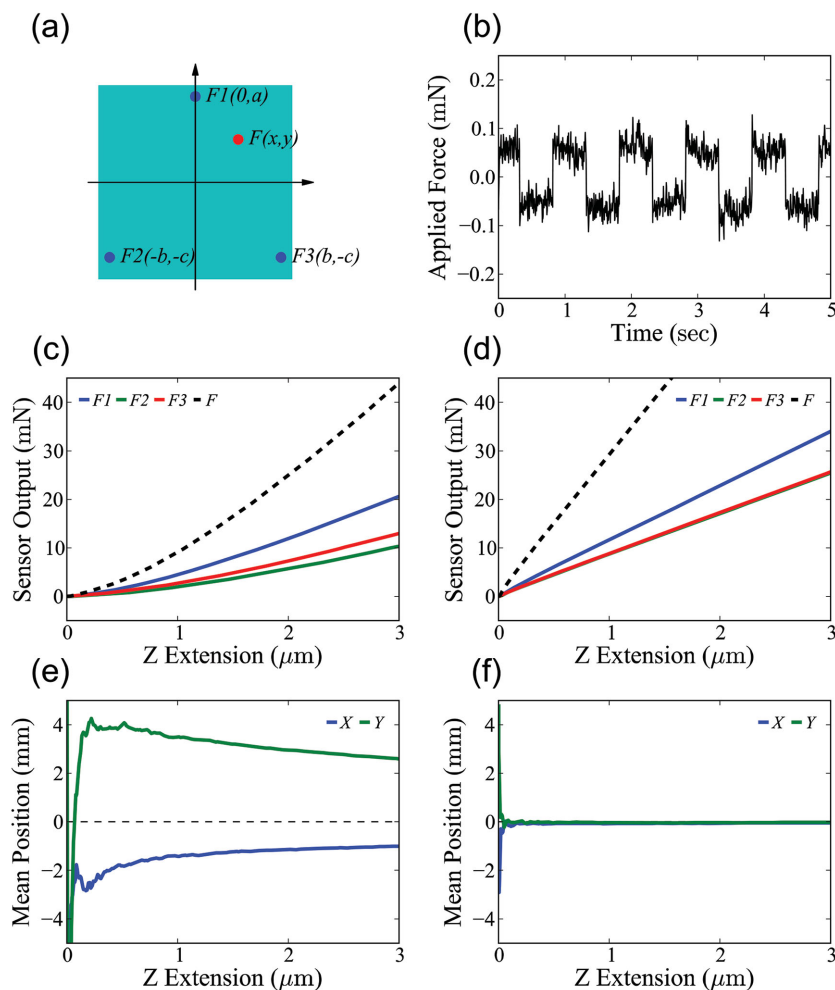


**Figure 3.** Leveling experiment with PPA. a) Coordinates of a three-point force sensor and effective force. b) High resolution total force measurement with applied square wave voltage across the  $z$  piezo. Force noise in standard deviation is less than 20  $\mu\text{N}$  at 100 Hz bandwidth. c,d) Force–distance curves for unlevelled and leveled cases, respectively. e,f) Measured position of the effective force for unlevelled and leveled cases, respectively.



$$X = b \cdot (f_3 - f_2) \quad (10)$$

$$Y = a \cdot f_1 - c \cdot (f_2 + f_3) \quad (11)$$

where  $f_i = F_i / F$  ( $i = 1, 2, 3$ )

The effective force position is a function of the force ratios. If denominator  $F$  is too small to measure, then the positions have large errors. Thus, the force sensors must have high sensitivity to enhance leveling accuracy. As shown in Figure 3b, we achieved high sensitivity using piezoresistive sensors and implementing optimized signal conditioning circuits. The measured total force is sufficient to resolve a 0.13 mN force difference applied by the square wave voltage across the  $z$  piezo, and the standard deviation of force noise is less than 20  $\mu$ N at 100 Hz bandwidth, and measurable up to 1 N.

By means of three-point force sensing structures and the direction feedback leveling with bisection method, we conducted PPA leveling on a silicon substrate. When PPA is unlevelled with regards to the substrate, the total force is varied nonlinearly as shown in Figure 3c according to the  $z$  scanner extension due to widening of the contact area. Furthermore, in Figure 3d, the effective force position deviates away from the center, here defined as the origin of the PPA. The front part of the position curves in Figure 3d shows large errors because the total force is too small to discriminate from the measurement

noise, which leads to an error in the calculation of the position. In our experiment, a total force of more than 1 mN is required for measurement reliability. If we increase the  $z$  extension length, then the position gets closer to the origin, which can be inferred from the simulation in Figure 2. Therefore, the total force should be maintained as a constant during the leveling process as in the constant force case in Figure 2. Once leveling is completed, then total force curve shows a linear response to the  $z$  extension, and the effective force positions become zero as represented in Figure 3e,f).

In order to verify leveling accuracy, we performed polymer pen lithography on a Au-coated silicon substrate using 16-mercaptohexadecanoic acid (MHA). As shown in Figure 4a,  $7 \times 7$  patterns were fabricated per one tip with sequential operation of various conditions of dwell time and  $z$  extension length. The image is obtained by lateral force mode of AFM and the scan size is 95  $\mu$ m. Since PPA consists of  $125 \times 125$  tips, 15 625 sets were duplicated in a  $1 \times 1$  cm<sup>2</sup> area.  $4 \times 4$  sets are displayed in the 310  $\mu$ m scan size AFM image shown in Figure 4b. The distance between pattern sets is 80  $\mu$ m which is induced from the tip spacing. To evaluate leveling accuracy, we obtained scanning electron microscope images along the full distance of the PPA, and edge lengths of two selected patterns which have average sizes of 5.5 and 4  $\mu$ m are shown in Figure 4c. The slopes of linear fitting of 5.5 and 4  $\mu$ m patterns are  $0.001^\circ$

and  $0.002^\circ$ , respectively, demonstrating that the leveling is successful. Edge length variations are measured as  $5.5 \pm 0.3$  and  $4.0 \pm 0.4$   $\mu$ m and their standard deviations are 0.15 and 0.2  $\mu$ m for each 5.5 and 4.0  $\mu$ m pattern, respectively. This error scale is comparable to that of Xie et al. who employed a novel concept of tip arrays.<sup>[11]</sup> Because our PPA has a flattop width of 300 nm (Figure S2, Supporting Information), the edge length variation is larger than that of Liao et al. who obtained a value of  $2.54 \pm 0.05$   $\mu$ m.<sup>[10]</sup> As proof-of-principle, it is possible to achieve better resolution if one combines this leveling method with precisely fabricated tip arrays. Importantly, in our approach, the entire leveling process is completed within 2 min in an automated manner, as described in the Experimental Section. This speed and functionality can lead to significant improvement toward realizing the concept of “desktop nanofabrication.”

### 3. Conclusion

In conclusion, we have demonstrated a new leveling method based on multipoint force detection structures and a direction feedback leveling algorithm. This new platform is capable of conducting precise, easy, and quick leveling for extensive

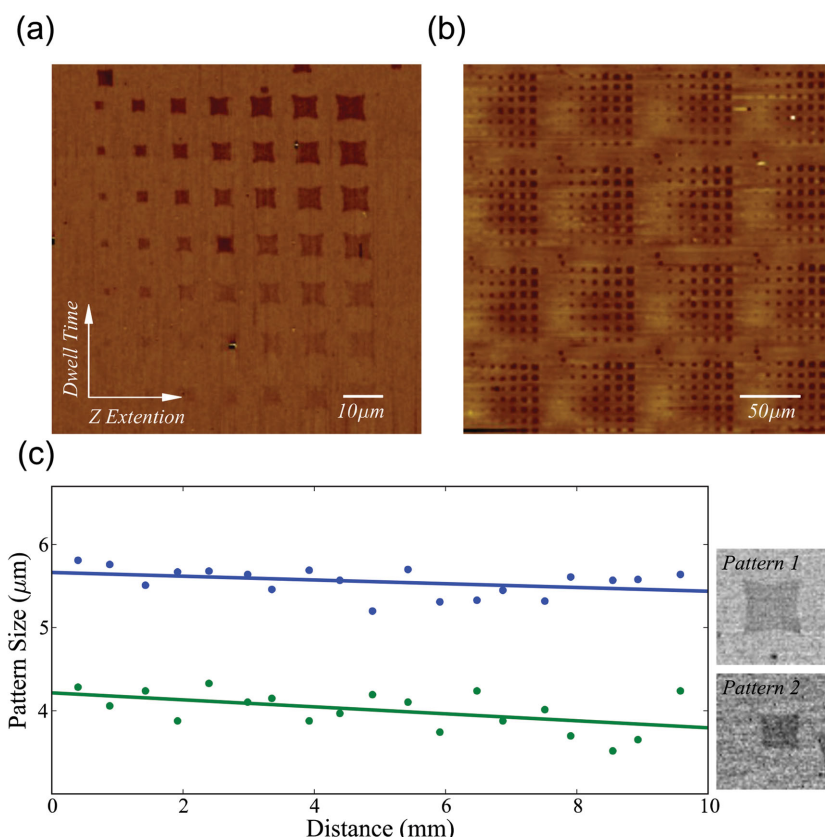


**Figure 4.** PPL patterning with MHA. a) AFM lateral force image with 95  $\mu$ m scan size.  $7 \times 7$  patterns are produced in sequential order with dwell time and  $z$  extension variation. b)  $4 \times 4$  repeated pattern sets with 310  $\mu$ m scan size lateral force image. c) Edge length variation of two selected patterns along 1 cm distance. Leveling is achieved with  $0.001^\circ$  order.

SPL techniques by means of the force-sensor-integrated tip holder and automated leveling algorithm. As proof-of-principle, we demonstrated a PPL patterning scheme. Resulting fabricated features show  $0.001^\circ$  slope of edge length variation along 1 cm length tip arrays. In addition, this method reduces the leveling time down to 2 min. With a simple operating principle and wide expandability, this new leveling method is a promising technique for “desktop nanofabrication.”

## 4. Experimental Section

**Preparation and Characterization of Dot Arrays:** Polymer pen arrays with 15625 pens and 80  $\mu\text{m}$  separation between tips were prepared from PDMS (Sylgard 184, Dow Corning Corp.). Briefly, a 10:1 mixing ratio of elastomer base and curing agent was used to prepare the PDMS solution, which was poured into the microfabricated silicon mold. A glass support was subsequently placed on top of the PDMS mold, which was then cured for 2 h at  $85^\circ\text{C}$ . 100  $\mu\text{L}$  of EtOH solution containing  $10 \times 10^{-3}\text{ M}$  MHA was poured onto the cured PDMS and dried for 10 min. The polymer pen arrays were mounted onto a commercial AFM system (Park Systems, NX20) which is housed in a homemade glovebox and exposed to 50% relative humidity. MHA was patterned on a Si(100)/SiO<sub>x</sub> wafer coated with  $\approx 10\text{ nm}$  thick Au layer by ion sputtering (HOYEON Tech. Co., LTD) for 5 min with 20 mA current. Lithography was conducted by integrated software in AFM.

**Automatic Direction Feedback Leveling with Bisection Method:** Automatic leveling is achieved by integrated software XEP in the AFM. A probe attached to the sensor block is approached by moving the z stepping motor to the sample substrate until the total force reaches a defined threshold. Once the approach is finished, then the tilt direction between the probe and sample is directly obtained by calculating position signals  $X$  and  $Y$  from the force signals  $F_1$ ,  $F_2$ ,  $F_3$ , and  $F$ . The probe is retracted to a certain height in order to prevent crash. A 2-axis tilting stage is moved in the opposite direction of the current tilt direction with predefined initial steps. Then approach, measure, retract, and tilt processes are iterated with a half of the previous tilting steps. After several iterations, once the tilting steps reach below a predefined stop step, then leveling is finally finished. The total force threshold, initial tilt steps, stop steps are tunable according to the probe types and leveling accuracy. A bisection algorithm converges to the acceptable tilt angles very quickly in both the  $x$  and  $y$  directions simultaneously. Thus, leveling time is much shorter than the method of determining the peak of the total force which requires equally spaced steps in iterations and sequential operation in  $x$  and  $y$  direction sweep.

## Supporting Information

Supporting Information is available from the Wiley Online Library or from the author.

## Acknowledgements

H. Noh and G.-E. Jung contributed equally to this work. This work was supported by the National Research Foundation (NRF-NRFF2011–01), and the National Medical Research Council (NMRC/CBRG/0005/2012) to N.J.C. This work was also supported in part by the Basic Science Research Program through the National Research Foundation of Korea (NRF) funded by the Ministry of Science, ICT & Future Planning (Grant No. 2013R1A1A2011526) and Advanced Technology Center (ATC) Program funded by the Ministry of Trade, Industry & Energy (Grant No. 10045812) to S.-J.C.

- [1] H. T. Soh, K. W. Guarini, C. F. Quate, *Scanning Probe Lithography*, Vol. 7, Springer, USA, **2001**.
- [2] G. Binnig, C. F. Quate, C. Gerber, *Phys. Rev. Lett.* **1986**, *56*, 930.
- [3] X. Xie, H. Chung, C. Sow, A. Wee, *Mater. Sci. Eng., R* **2006**, *54*, 1.
- [4] R. D. Piner, J. Zhu, F. Xu, S. Hong, C. A. Mirkin, *Science* **1999**, *283*, 661.
- [5] K. Salaita, Y. Wang, J. Fragala, R. A. Vega, C. Liu, C. A. Mirkin, *Angew. Chem.—Int. Ed.* **2006**, *45*, 7220.
- [6] F. Huo, Z. Zheng, G. Zheng, L. R. Giam, H. Zhang, C. A. Mirkin, *Science* **2008**, *321*, 1658.
- [7] F. Huo, G. Zheng, X. Liao, L. R. Giam, J. Chai, X. Chen, W. Shim, C. A. Mirkin, *Nat. Nanotechnol.* **2010**, *5*, 637.
- [8] W. Shim, A. B. Braunschweig, X. Liao, J. Chai, J. K. Lim, G. Zheng, C. A. Mirkin, *Nature* **2011**, *469*, 516.
- [9] X. Liao, K. A. Brown, A. L. Schmucker, G. Liu, S. He, W. Shim, C. A. Mirkin, *Nat. Commun.* **2013**, *4*, 2103.
- [10] X. Liao, A. B. Braunschweig, C. A. Mirkin, *Nano Lett.* **2010**, *10*, 1335.
- [11] Z. Xie, Y. Shen, X. Zhou, Y. Yang, Q. Tang, Q. Miao, J. Su, H. Wu, Z. Zheng, *Small* **2012**, *8*, 2664.
- [12] J. Haaheim, V. Val, J. Bussan, S. Rozhok, J. W. Jang, J. Fragala, M. Nelson, *Scanning* **2010**, *32*, 49.
- [13] Z. Liu, X. Chen, Y. Zhang, J. Weaver, C. J. Roberts, *Appl. Phys. Lett.* **2012**, *101*, 173112.
- [14] A. B. Braunschweig, F. Huo, C. A. Mirkin, *Nat. Chem.* **2009**, *1*, 353.
- [15] J. M. Hong, F. M. Ozkeskin, J. Zou, *J. Micromech. Microeng.* **2008**, *18*, 015003.
- [16] D. Qin, Y. Xia, A. J. Black, G. M. Whitesides, *J. Vac. Sci. Technol., B: Microelectron. Nanometer Struct.* **1998**, *16*, 98–103.
- [17] J. Chai, *Proc. Natl. Acad. Sci. U.S.A.*, **2010**, *107*, 20202.
- [18] F. Brinkmann, M. Hirtz, A. M. Greiner, M. Weschenfelder, B. Waterkotte, M. Bastmeyer, H. Fuchs, *Small* **2013**, *9*, 3266.
- [19] S. Bian, J. He, K. B. Schesing, A. B. Braunschweig, *Small* **2012**, *8*, 2000.
- [20] D. J. Eichelsdoerfer, X. Liao, M. D. Cabezas, W. Morris, B. Radha, K. A. Brown, L. R. Giam, A. B. Braunschweig, C. A. Mirkin, *Nat. Protoc.* **2013**, *8*, 2548.
- [21] X. Zhong, N. A. Bailey, K. B. Schesing, S. Bian, L. M. Campos, A. B. Braunschweig, *J. Polym. Sci., Part A-1: Polym. Chem.* **2013**, *51*, 1533.
- [22] X. Liao, A. B. Braunschweig, Z. Zheng, C. A. Mirkin, *Small* **2010**, *6*, 1082.

Received: December 17, 2014  
Revised: March 23, 2015  
Published online: June 16, 2015